

**AROMATIZATION OF *n*-OCTANE OVER Pt-Sn/KL CATALYSTS:
ACTIVITY AND REGENERATION**



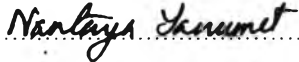
Worarat Charoennam

A Thesis Submitted in Partial Fulfilment of the Requirements
for the Degree of Master of Science
The Petroleum and Petrochemical College, Chulalongkorn University
in Academic Partnership with
The University of Michigan, The University of Oklahoma,
Case Western Reserve University and Institut Français du Pétrole
2008

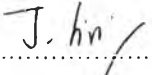
512011


Thesis Title: Aromatization of *n*-Octane over Pt-Sn/KL Catalysts:
Activity and Regeneration
Program: Petroleum Technology
Thesis Advisors: Dr. Siriporn Jongpatiwut
Assoc. Prof. Thirasak Rirksomboon
Prof. Somchai Osuwan
Prof. Daniel E. Resasco

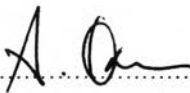
Accepted by the Petroleum and Petrochemical College, Chulalongkorn University, in partial fulfilment of the requirements for the Degree of Master of Science.


..... College Director
(Assoc. Prof. Nantaya Yanumet)

Thesis Committee:

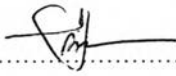

.....
(Dr. Siriporn Jongpatiwut)


.....
(Assoc. Prof. Thirasak Rirksomboon)


.....
(Prof. Somchai Osuwan)


.....
(Prof. Daniel E. Resasco)


.....
(Dr. Thammanoon Sreethawong)


.....
(Assoc. Prof. Tawan Sooknoi)

ABSTRACT

4973011063 Petroleum Technology

Worarat Charoennam: Aromatization of *n*-Octane over Pt-Sn/KL Catalysts: Activity and Regeneration

Thesis Advisors: Dr. Siriporn Jongpatiwut, Prof. Daniel E. Resasco, Assoc. Prof. Thirasak Rirksomboon and Prof. Somchai Osuwan, 84 pp.

Keywords: *n*-Octane Aromatization/ Pt-Sn Catalyst/ Catalyst Regeneration

Platinum supported on KL zeolite (Pt/KL) is an efficient catalyst for the aromatization of *n*-hexane into benzene, but is not as effective for *n*-octane aromatization. The product distribution shows small quantities of C8-aromatics but high amounts of benzene and toluene, which are undesired products from the secondary hydrogenolysis reaction. In previous studies, using nano-crystalline KL zeolite (NCL) and the addition of Sn enhanced the activity and selectivity toward C8 aromatics. The advantage of using the NCL is to reduce the diffusion limitations while that of the Sn addition is to break the Pt ensemble by forming the Pt-Sn alloy phase; hence, the hydrogenolysis reaction is inhibited. However, the Pt-Sn alloy may be destroyed during the catalyst regeneration. Therefore, in this work, the combination of using NCL zeolite with the addition of Sn on Pt/KL was studied. It was found that the addition of Sn improved the catalytic activity and selectivity on both Pt/COM and Pt/NCL. However, the PtSn/COM gave higher C8 aromatics than PtSn/NCL. This could be because PtSn/COM has higher fraction of PtSn alloy phase than PtSn/NCL. The effects of regeneration temperature (300-500°C), time (15 min-2 h) and air flow rate (10-40 ml/min) on Pt-Sn alloy over COM were also studied. Among the conditions tested, the catalyst regenerated with an air flow rate of 20 ml/min at 400°C for 1 h exhibits the highest degree of PtSn alloy and low residual coke contents, leading to the highest catalytic activity and selectivity in the 2nd cycle which is close to the those observed on the fresh Pt-Sn/COM catalyst.

ACKNOWLEDGEMENTS

This thesis work is partially funded by the Petroleum and Petrochemical College; the National Center of Excellence for Petroleum, Petrochemicals, and Advanced Materials, Thailand; and the Grant for Development of New Faculty Staff, Chulalongkorn University.

I would like to express my greatest appreciation to Dr. Siriporn Jongpatiwut, Assoc. Prof. Thirasak Rirksomboon, Prof. Somchai Osuwan, and Prof. Daniel E. Resasco for their guidance, assistance, and the opportunity to do research at the University of Oklahoma. Their professionalism and expertise has inspired me in many ways while writing throughout my research. I would also like to thank all friends and staff at the PPC for their help and support.

It is my pleasure to acknowledge Dr. Supak Trakarnroek and Dr. Pisan Chungchamroenkit for giving me priceless knowledge and helping me with the problems that I have stumbled upon during my research. I would also like to thank Mr. Robert Wright for his valuable advice in writing papers and thesis. Special thanks also go to Jongpatiwut's group for helping me operate the laboratory.

My deepest appreciation goes to Air, Q, and Phueng for making my transition from Thailand to United States as smooth as possible and giving excellent suggestion. My appreciation also goes to Kitt and Emma for their allowing me to stay in their home during my stay at the University of Oklahoma. I would also like to thank Ming for showing me the American culture as well as fine tuning my English speaking and writing skills.

Special gratitude goes to all of my family who have supported me throughout my life, these people have been with me through great and bad times and shared every moment that I have encountered. Without these special people, I would not have been able to achieve my Master's degree in Petroleum Technology. I am grateful for everything they have given me.

TABLE OF CONTENTS

	PAGE
Title Page	i
Abstract (in English)	iii
Abstract (in Thai)	iv
Acknowledgement	v
Table of Contents	vi
List of Tables	x
List of Figures	xi
 CHAPTER	
I INTRODUCTION	i
 II LITERATURE REVIEW	
2.1 Catalytic Reforming	4
2.1.1 <i>o</i> -Xylene	5
2.1.2 Ethylbenzene	5
2.2 Catalysts for Aromatization of <i>n</i> -Alkane	6
2.2.1 Molecular Die (geometric) Effects	6
2.2.2 Preorganization of <i>n</i> -Hexane for Ring Closure	6
2.2.3 Electronic Effects	6
2.2.4 Inhibition of Bimolecular Pathway	7
2.2.5 Stabilization of Small Pt Clusters	7
2.3 The Structure of LTL Zeolite	8
2.4 Synthesis of KL Zeolites	9
2.5 The Effect of Additional Promoter into Pt/KL Catalyst	11
2.6 Catalyst Deactivation	16

CHAPTER	PAGE
2.6.1 Poisoning	17
2.6.2 Fouling	18
2.6.2.1 Coking	18
2.6.2.2 Metal Deposition	21
2.6.3 Thermal Degradation	22
2.6.3.1 Sintering of Metals	22
2.6.3.2 Sintering of Supports	23
2.6.3.3 Thermal Degradation of Supported Catalysts	23
2.6.4 Loss of Catalytic Phase by Vapour Transport	24
2.6.5 Mechanical Failure of Catalysts	24
2.7 Prevention of Catalyst Deactivation	24
2.8 Regeneration of Deactivated Catalysts	26
2.8.1 Regeneration Parameters	27
2.8.1.1 Temperature	27
2.8.1.2 Heating Rate	29
2.8.1.3 Time	29
 III EXPERIMENTAL	 31
3.1 Material	31
3.1.1 Chemicals	31
3.1.2 Gases	31
3.2 Equipment	32
3.3 Methodology	32
3.3.1 Synthesis of the Nano-crystalline KL Zeolites	32
3.3.2 Catalyst Preparation	33
3.3.3 Characterization of Synthesized KL Zeolites and Catalyst	34
3.3.3.1 X-Ray Diffraction (XRD)	34

CHAPTER	PAGE
3.3.3.2 Dynamic Light Scattering (DLS)	34
3.3.3.3 Hydrogen Chemisorption	35
3.3.3.4 Transmission Electron Microscopy (TEM)	35
3.3.3.5 Temperature Programmed Reduction (TPR)	35
3.3.3.6 X-Ray Photoelectron Spectroscopy (XPS)	36
3.3.3.7 Temperature Programmed Oxidation (TPO)	36
3.3.4 Catalytic Activity Testing	37
3.3.5 Regeneration in Air	38
3.3.5.1 Pretreatment	38
3.3.5.2 Coke Oxidation	39
3.3.5.3 Final Reduction	39
3.3.6 The Product of <i>n</i> -Octane Aromatization Analysis	39
IV RESULTS AND DISCUSSION	40
4.1 Synthesis of the Nano-crystalline KL Zeolites	40
4.2 Characterization of the Fresh Catalysts	42
4.3 Catalytic Activity Testing: <i>n</i> -Octane Aromatization	48
4.4 Regeneration in Air of deactivated 1Pt1Sn/COM Catalysts	54
4.4.1 Effect of Regeneration Temperature	54
4.4.1.1 Catalytic Activity Measurement	54
4.4.1.2 Characterization of Catalysts	59
4.4.2 Effect of Regeneration Time	65
4.4.1.1 Catalytic Activity Measurement	65
4.4.1.2 Characterization of Catalysts	67

CHAPTER	PAGE
4.4.3 Effect of Regeneration Air Flow Rate	69
4.4.3.1 Catalytic Activity Measurement	69
4.4.3.2 Characterization of Catalysts	72
V CONCLUSIONS AND RECOMMENDATIONS	75
REFERENCES	76
CURRICULUM VITAE	84

LIST OF TABLES

TABLE	PAGE	
2.1	Prevention of catalyst deactivation	25
3.1	List of mono- and bi- metallic Pt-Sn/KL catalysts investigated	34
3.2	Regeneration Conditions	38
4.1	The comparison between the particle size of COM and NCL measured by DLS method	41
4.2	Analysis of Fresh and Spent Catalysts	43
4.3	Deconvolution of TPR profile of bimetallic Pt-Sn/KL catalysts	45
4.4	Binding energies and relative intensities of different species from curve-fitted XPS spectra of various catalysts	47
4.5	<i>n</i> -Octane conversion and product distribution over 1Pt/COM, 1Pt/NCL, 1Pt1Sn/COM, 1Pt1Sn/NCL, and 1Pt0.6Sn/NCL catalysts tested for <i>n</i> -octane aromatization after 550 min time on stream; Reaction condition: temperature = 500°C, pressure = 1 atm, WHSV = 5 h ⁻¹ , H ₂ :HC = 6:1	49
4.6	Binding energies and relative intensities of different species from curve-fitted XPS spectra of various catalysts	63
4.7	TPO analysis of spent and regenerated 1Pt1Sn/COM catalysts at different regeneration temperatures	64
4.8	TPO analysis of spent and regenerated 1Pt1Sn/COM catalysts at different regeneration times	69
4.9	TPO analysis of spent and regenerated 1Pt1Sn/COM catalysts at different regeneration air flow rates	73

LIST OF FIGURES

FIGURE	PAGE
2.1 Schematic of <i>o</i> -xylene.	5
2.2 Schematic of phthalic anhydride.	5
2.3 Schematic of dehydrogenation of ethylbenzene	6
2.4 Schematic of L zeolite structure.	8
2.5 SEM image of hockey puck KL zeolite with the size of 40,000 times (Verduijn <i>et al</i> , 2001).	10
2.6 Conceptual model of fouling, crystallite encapsulation and pore plugging of a supported metal catalyst due to carbon deposition.	19
2.7 Relationship between catalyst activity loss and coke deposition with during of run.	20
2.8 Temperature programmed oxidation (TPO) profiles of coke deposits left over the Pt/KL-VPI catalyst after 9 h on stream during <i>n</i> -hexane (thin line) and <i>n</i> -octane aromatization (heavier line). Reaction condition: 500°C, H ₂ / <i>n</i> -C ₆ (or <i>n</i> -C ₈) molar ratio 6:1, WHSV 5 h ⁻¹ .	21
3.1 Schematic diagram of the experimental set-up for <i>n</i> -alkane aromatization.	37
4.1 XRD patterns of nano-crystalline KL zeolite (NCL) and commercial KL zeolite (COM).	40
4.2 TEM image of synthesized nano-crystalline KL zeolite (NCL) at 175°C for 8 h.	41
4.3 FTIR spectra of nano-crystalline KL zeolites obtained at aging time of 17 h and crystallization time of 8 h synthesized by microwave hydrothermal treatment compared to that of commercial KL zeolite (COM).	42

FIGURE	PAGE
4.4 TEM images of metal size distribution obtained by TEM of the mono- and bi- metallic Pt-Sn/KL catalysts.	43
4.5 TPR profiles of the different Sn/Pt ratio of bimetallic Pt-Sn catalysts prepared by vapor phase co-impregnation.	45
4.6 Pt4f XPS spectra of 1Pt/COM and 1Pt1Sn/COM after hydrogen treatment for 1 h at 500°C (reduced).	47
4.7 The variations of (a) <i>n</i> -octane conversion (b) total aromatics selectivity and (c) C8-aromatics selectivity with time on stream (Catalyst: 1Pt/COM and 1Pt/NCL. Reaction condition; temperature = 500°C, pressure = 1 atm, WHSV = 5 h ⁻¹ , H ₂ :HC = 6:1).	50
4.8 The variations of <i>n</i> -octane conversion and C8-aromatics selectivity on mono- and bi- metallic Pt-Sn supported on (a), (c) COM and (b),(d) NCL with time on stream. (Reaction condition; temperature = 500°C, pressure = 1 atm, WHSV = 5 h ⁻¹ , H ₂ :HC = 6:1).	52
4.9 The variation of <i>n</i> -octane conversion at 500°C without regeneration in air.	56
4.10 The <i>n</i> -octane conversion after 370 min on stream of regenerated catalysts at various regeneration temperatures (300-500°C).	55
4.11 The C8-aromatics selectivity after 370 min on stream of regenerated catalysts at various regeneration temperatures (300-500°C).	57
4.12 The total aromatics selectivity after 370 min on stream of regenerated catalysts at various regeneration temperatures (300-500°C).	58

FIGURE	PAGE
4.13 The EB/OX ratio after 370 min on stream of regenerated catalysts at various regeneration temperatures (300-500°C).	59
4.14 TPR profiles of regenerated catalysts at various regeneration temperatures (300-500°C).	60
4.15 Pt4f XPS spectra of 1Pt/COM, 1Pt1Sn/COM and regenerated 1Pt1Sn/COM catalyst in air at 400°C after hydrogen treatment for 1 h at 500°C (reduced).	62
4.16 The <i>n</i> -octane conversion after 370 min on stream of regenerated catalysts at various regeneration times (15-120 min).	65
4.17 The C8-aromatics selectivity after 370 min on stream of regenerated catalysts at various regeneration times (15-120 min).	66
4.18 The total aromatics selectivity after 370 min on stream of regenerated catalysts at various regeneration times (15-120 min).	66
4.19 The EB/OX ratio after 370 min on stream of regenerated catalysts at various regeneration times (15-120 min).	67
4.20 TPR profiles of regenerated catalysts at various regeneration times (15-120 min).	68
4.21 The <i>n</i> -octane conversion after 370 min on stream of regenerated catalysts at various regeneration air flow rates (10-40 ml/min).	70
4.22 The C8-aromatics selectivity after 370 min on stream of regenerated catalysts at various regeneration air flow rates (10-40 ml/min).	70

FIGURE		PAGE
4.23	The total aromatics selectivity after 370 min on stream of regenerated catalysts at various regeneration air flow rates (10-40 ml/min).	71
4.24	The EB/OX ratio after 370 min on stream of regenerated catalysts at various regeneration air flow rates (10-40 ml/min).	71
4.25	TPR profiles of regenerated catalysts at various regeneration air flow rates (10-40 ml/min).	72